

Modeling of the RHC System with Bond Graphs Approach

Abdelatif Merabtine^a, Riad Benelmir^{b,*}

^a Ecole Normale Supérieure de Cachan - LMT, Cachan, France, 94235

^b Lorraine University - LERMAB, Vandoeuvre-lès-Nancy, France, 54506

Abstract

In this work, a simplified graphical modeling tool, which in some extent can be considered in halfway between detailed physical and Data driven dynamic models, has been developed. This model is based on Bond Graphs approach. This approach has the potential to display explicitly the nature of power in a building system, such as a phenomenon of storage, processing and dissipating energy such as Heating, Ventilation and Air-Conditioning (HVAC) systems. In this paper, thermal behavior of an elementary referential building configured with two similar adjacent spaces has been modeled in order to assess the performance of the combined Radiant Heating and Cooling (RHC) systems. The thermal simulation of the building has been performed by using the Bond Graphs modeling approach, where both temperatures and heat flux annual profiles, according to the radiative heat exchange, have been calculated. Comparison with TRNSYS software results has also been made. It was found that the RHC system is able to meet energy demand of the building insuring a good thermal comfort level.

Keywords: Building Energy Efficiency, Bond Graphs modeling, HVAC.

1. Introduction

The rapidly growing energy use gave rise to exhaustion of energy resources and heavy environmental impact. The building sector alone stands for the most energy consuming sector in France with 43% of final energy consumption and 25% of greenhouse gases emission [1]. Thus, efforts should be taken in new buildings construction and existent buildings thermal renovation in order to satisfy low energy building criterions [2]. To meet this objective, it is necessary to use a representation for building analysis in order to model both qualitative and quantitative dynamic aspects. Nowadays, several software packages such as ESP, DOE2, PLEIADES, TAS [3] have been developed to carry out parametrical studies during the design of low energy efficient buildings. Some commercial software packages are based on a simplified steady state models. These ones benefit in reliability and time, but are poor in accuracy, so they are often applied at the preliminary design stage. Detailed dynamic models benefit in accuracy. They are often applied in the analysis of annual energy consumption and performance of building HVAC systems. Regarding the building system as a whole where dynamic exchanges of heat and mass transfer occur, the models can be mainly categorized into physical models, data driven models and gray models.

Physical modeling, also called forward modeling, begins with a description of the building system or component of interest and defines the building according to its physical description. Most simulation models are based on these principals, such as EnergyPlus [4], DOE-2 [5], TAS [6], ESP-r [7] and TRNSYS [8]. These models require a large number of parameters as inputs for the simulation and the process of collecting a physical description is time consuming. Data driven dynamic models are often described by regression techniques [9, 10] where a standard parametric model is adapted to measured data obtained from an experiment on the building process. In this kind of models, it is generally necessary to acquire data over a long period of time with widely varying conditions in order to train the models for accurate predictions under all conditions. Also, these models do not reflect any specific physical structure. Gray models [11,12,13] are a combination of models based on physical laws and with a parametric identification procedure using a limited number of parameters having a definite physical meaning. The thermal network model using electrical analogy parameters is an example of gray models. Gray models can represent the physical properties of building system and predict its thermal behavior and consumption and are suitable for nonlinear processes such as solar radiation. They are considered as simplified physical models which can represent properly the physical properties of the building system. Therefore, much of such simplified models are commonly developed to overcome the heaviness of detailed

* Corresponding author. Tel.: +33147407467

Fax: +33147407464; E-mail: amerabti@ens-cachan.fr

© 2013 International Association for Sharing Knowledge and Sustainability

DOI: 10.5383/ijtee.05.02.007

physical models. However, there are few unified models whatsoever detailed physical or gray models which can be used for representing and analyzing different building sub-systems simultaneously [13].

The aim of this paper is to develop the dynamic model of the RHC system based on the Bond Graphs approach. A Bond Graphs is a graphical representation of a physical dynamic system. A final simulation tool is of modular technological level. This tool provides a comprehensive graphical user interface allowing future extensions.

2. Bond Graphs methodology

The Bond Graphs technique is based on a graphical formalism. It is well suited for modeling physical processes and multidisciplinary dynamic engineering systems including features and components involved in different energy domains. This approach is founded on a systematic and common way representation of power flow between the model's components. Paynter [14] started the Bond Graphs formalism and used it for modeling dynamic multiport systems. He suggested that energy and power are the fundamental dynamic variables which characterize all physical interactions.

In Bond Graphs modeling, the interaction between two components is modeled by a bond with a semi-arrow in the end. The power is represented as product of two physical quantities, one extensive, the other intensive. These two power conjugated variables are called *effort* and *flow* and are denoted by the letters e and f (Fig. 3).

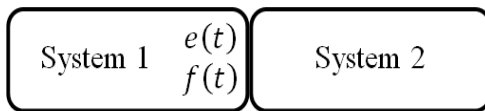


Fig. 1. Bond Graphs link.

The selection of these two physical quantities is specific for each physical domain. For instance, in electrical domain, we use the voltage u as effort variable and the current i as flow variable. In thermal domain, the effort variable is represented by the temperature T and the flow variable by the heat flow \dot{Q} . However, the product “temperature by heat flow” is not the power transferred between ports. This has conducted researchers to introduce the “pseudo-bond graphs” (PBG) for modeling thermal systems. The advantage of PBG is the fact that it facilitates the modeling of the thermal systems overcoming the non-linear thermal problems.

A classification of Bond Graphs elements can be made up by the number of ports. Ports are placed where interactions with other processes take place. There are one port elements symbolizing inertial element (I), capacitive element (C), resistive element (R), effort source (Se) and flow source (Sf), and two ports elements representing transformer element (TF) and gyrator element (GY). The elements I, C, and R are passive elements because they convert the supplied energy into stored or dissipated energy. The sources Se and Sf are active elements because they supply power to the system. The bonds are inter-linked by two types of junctions: 0-junction and 1-junction which serve to connect I, C, R, and source elements. At the 0-junction, the flow adds up to zero while all efforts are equal, and at the 1-junction all effort variables add up to zero while all flows are equal. The concept of causality is an important concept embedded in Bond Graphs theory. This refers to cause and effect relationship. Thus, as part of the Bond Graphs modeling process, a causality assignment is implicitly introduced.

In order to explain the PB G modeling approach, we propose to model the heat loss through a homogeneous wall constituting the building envelope. The absolute temperature T may be chosen as an effort variable and heat flow as a flow variable \dot{Q} .

Lumped parameter assumption is usually adopted in such a case. This is realized by splitting the wall into a number of layers, where, temperature and the thermo physical properties are assumed homogeneous (Fig. 2). Each layer stores and conducts heat simultaneously. The external ones are subject to convection heat exchange with inside and outside surrounding.

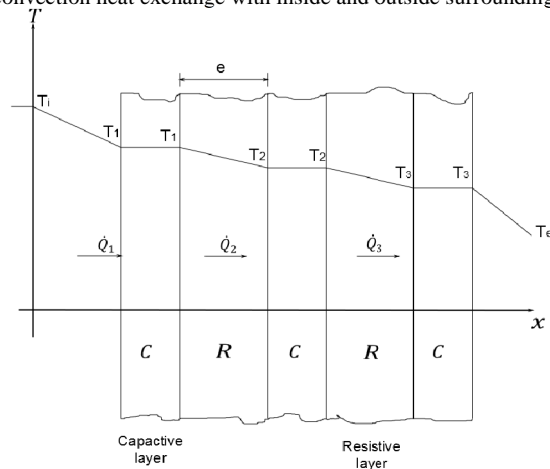


Fig. 2. Representation of the spitted wall

The PBG model representation of the heat conduction into the wall constituted of four layers is shown in Figure 3.

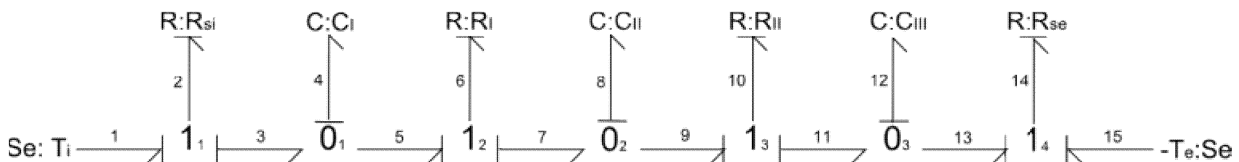


Fig.3. Numerated PBG model of the wall

Power bonds may join at one of two kinds of junctions: a “0” junction and a “1” junction. In a 0 junction, the flows and the efforts satisfy the equations (1) and (2):

$$\sum_{i=1}^n f_i = 0 \tag{1}$$

$$e_1 = e_2 = \dots = e_n \tag{2}$$

In a 1 junction, the flows and the efforts satisfy the equations (3) and (4):

$$f_1 = f_2 = \dots = f_n \tag{3}$$

$$\sum_{i=1}^n e_i = 0 \tag{4}$$

The *R* and *C* elements represent respectively, the thermal resistance and the thermal capacity, given by

$$R = \begin{cases} \frac{e_l}{\lambda A} & (\text{conduction}) \\ \frac{1}{hA} & (\text{convection}) \end{cases} \tag{5}$$

$$C = \rho e_l A c \tag{6}$$

e_l is the thickness of each layer, *λ* is the thermal conductivity of the material, *h* is the convection coefficient and *A* is the area of the layer.

The constitutive equations between the efforts and flows corresponding to *R* and *C*-elements are respectively given by:

$$e(t) = Rf(t) \tag{7}$$

$$e(t) = \frac{1}{C} \int f dt \tag{8}$$

T_i and *T_e* represent the indoor and outdoor temperatures.

For each layer inside the wall, the heat quantity is split in two parts: the first part is dissipated by conduction; modeled by a 1-junction related to *R*-element representing the conductive resistance, whereas the second part is stored by the layer; modeled by a 0-junction related to *C*-element representing the thermal capacity. Once written, the equations are given in the following matrix form:

$$\begin{bmatrix} -\left(\frac{1}{R_{st}} + \frac{1}{R_1 C_I}\right) & \frac{1}{R_1 C_{II}} & 0 \\ \frac{1}{R_1 C_{II}} & -\left(\frac{1}{R_1 C_{II}} + \frac{1}{R_2 C_{II}}\right) & \frac{1}{R_2 C_{III}} \\ 0 & \frac{1}{R_2 C_{III}} & -\left(\frac{1}{R_2 C_{III}} + \frac{1}{R_{se} C_{III}}\right) \end{bmatrix} \dot{X} + \begin{bmatrix} \frac{1}{R_{st}} & 0 \\ 0 & 0 \\ 0 & \frac{1}{R_{se}} \end{bmatrix} U \tag{9}$$

with:

$$U = \begin{pmatrix} T_1 \\ T_{1.5} \end{pmatrix} \equiv \begin{pmatrix} T_i \\ -T_e \end{pmatrix} \tag{10}$$

$$X = \begin{pmatrix} q_4 \\ q_8 \\ q_{12} \end{pmatrix} \equiv \begin{pmatrix} q_I \\ q_{II} \\ q_{III} \end{pmatrix} \tag{11}$$

where *q_I*, *q_{II}*, and *q_{III}* are the heat stored by three capacitive layers.

The system of differential equations (9) gives the heat flow in each layer, this allows obtaining the temperature profile inside the wall.

In the case of the thermo-fluid systems, we use the multi-energy Bond Graphs with two effort variables (temperature *T* and pressure *P*) and two flow variables (heat flux \dot{Q} and mass flow \dot{m} or volume flow rate \dot{V}) (Fig.4). The thermo-fluid system is decomposed in lumps, each lump being represented by the *C* element, called accumulator. The energy dissipation between the system's components is represented by the 2-ports *R* element, called restrictor.

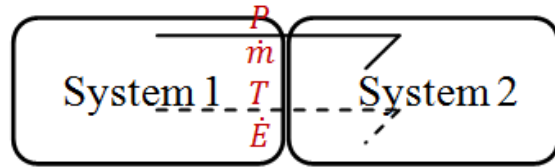


Fig. 4. Multi-energy Bond Graphs link

The Figure 5 shows PBG model of the basic component that accumulate energy *E* (for instance, ventilated room, storage tank, ...).

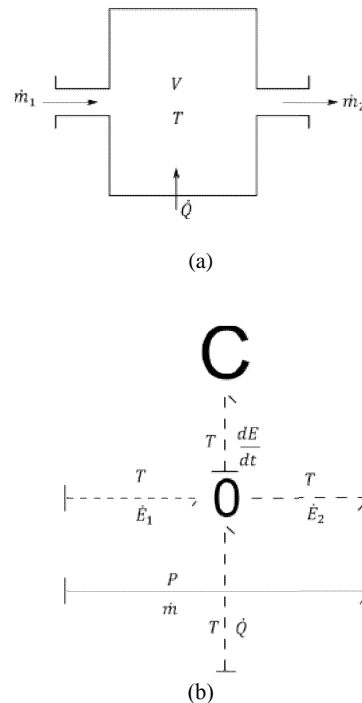


Fig. 5. Accumulator. (a) Energy storage; (b) PBG model

From the PBG representation, we derive the following equations :

$$\frac{dE}{dt} = \dot{E}_1 - \dot{E}_2 + \dot{Q} \tag{Energy balance} \tag{12}$$

$$\dot{m} = cste \tag{Mass balance} \tag{13}$$

The PBG model of the component that represents the energy dissipation is illustrated in Figure 6.

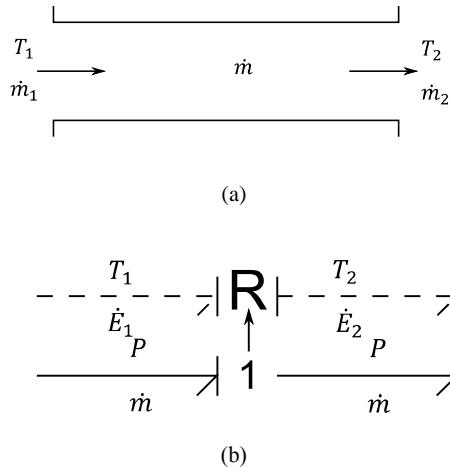


Fig. 6. Restrictor. (a) Energy dissipation through a pipe; (b) PBG model

As seen in Figure 6, we consider the continuity of the flow variables:

$$\dot{m}_1 = \dot{m}_2 \quad (14)$$

$$\dot{E}_1 = \dot{E}_2 \quad (15)$$

3. Bond Graphs methodology

The Radiant Heating and Cooling (RHC) systems aroused renewed interest because of their energy efficiency. They provide thermal comfort inside the building (uniformity of surface temperature and also low value of the operative temperature). In the case of the floor heating system (Fig. 7), the purpose is to maintain the upper surface of the floor at a maximum temperature of 27 °C. In fact, the heat exchange occurs mainly by radiation. Thanks to uniformity of heat distribution, this technique provides better thermal comfort than other types of heating systems [14].

Because of the high radiant heat output and the fact that occupants are close to the floor surface, it is an obvious choice to use the same system for cooling [15]. In this case, cooled water at about 15 °C circulates in the ceiling within circular copper tubes welded to steel plates (Fig. 8).

Various studies have been conducted on RHC systems: alone or coupled [16, 17]. Other authors were interested by the floor operating in the intermittent mode of heating (in winter) and cooling (in summer) [18, 19]. The performances of Direct Solar Floors (DSF) using a solar heating were investigated by Mokhtari *et al.* [18]. Results for an Algerian climate show the influence of the main sizing parameters and indicate that a large fraction of heating needs could be covered by solar energy. When cooling is considered (intermittent mode) an important decrease in resultant temperature can be achieved with a rather high fluid inlet temperature. The thermal behavior of chilled ceiling system and the interactions with walls, ventilated façade, internal loads and ventilation systems have been studied by Diaz *et al.* [19]. The commissioning test results show that the influence of surfaces temperature inside the room, especially the façades, is significant.



Fig. 7. The floor heating circuit



Fig. 8. The chilled ceiling plates

RHC systems were also studied including those that incorporate displacement ventilation [20] or dehumidification in the case of tropical climates [23]. Keblawi *et al.* [22] developed an optimized online supervisory control predictive tool for the chilled ceiling displacement ventilation system (CC/DV) to minimize energy consumption while creating the best Indoor Air Quality (IAQ) and thermal comfort. Hao *et al.* [23] conclude that, in comparison with a conventional all air systems, the combined system of chilled ceiling – displacement ventilation, and desiccant dehumidification saves 8.2 % of total primary energy consumption in addition to achieving better IAQ and thermal comfort. However, few studies considered the coupling of floor heating with chilled ceiling.

3.1 Dynamic model description

The constitutive elements of hydraulic systems are presented in Figure 9. In floor heating system (Fig. 9a), the heat exchange is convective through the hot water flowing within the polyethylene tube. The heat flow coming from the tube is, on one hand, dissipated by conduction to the ground (Q_g) and on the other hand, distributed to the concrete screed (Q_c) and then transferred to the inside air and adjacent walls by convection (Q_{conv}) and radiation (Q_{rad}). In the chilled ceiling system (Fig. 9b), the heat exchange is convective and radiation on both sides of the ceiling.

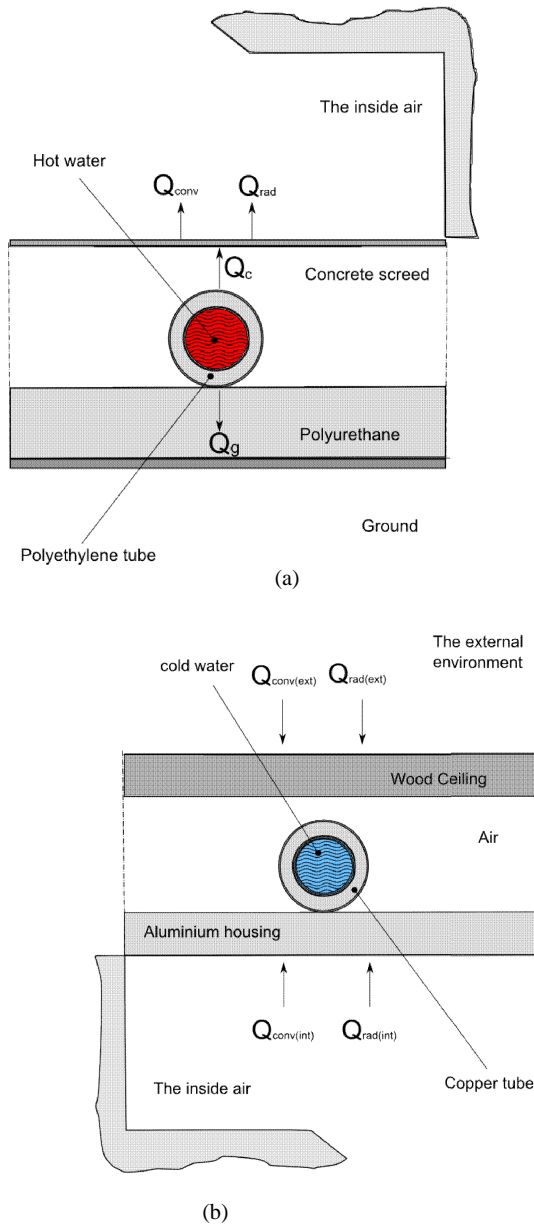


Fig. 9. Constitutive elements of the hydraulic systems. (a) Heating floor; (b) Chilled ceiling

For the incompressible flow case, the problem of causal switching with flow direction can be circumvented in a PBG in which a thermal model is actively coupled to a hydraulic model using special 2-port resistors [24]. A hydraulic model will be coupled to a thermal transport model in a dynamic way. The hydraulic model takes into account the energy transport by the fluid and the thermal model considers the internal energy transport and evaluates the fluid temperature [25].

In our casestudy, we use the following twostate variables(or displacement variables): the internal energy U and the volume V . With these variables, we use the pseudo-links corresponding to the pairsofvariables: the temperature T and enthalpy flow \dot{H} for the thermal model and pressure P and volume flow rate \dot{V} for the hydraulic model. The internal energy U is calculated in C-element representing the energy stored by the fluid.

Otherwise, the multiport-R element is used to calculate the volume flow rate \dot{V} and enthalpy flow \dot{H} through the tube. This element represents the energy dissipated along the tube.

Consider the control volume of Figure 6 with the internal water at instantaneous pressure P , absolute temperature T , volume V , and containing an internal energy U .

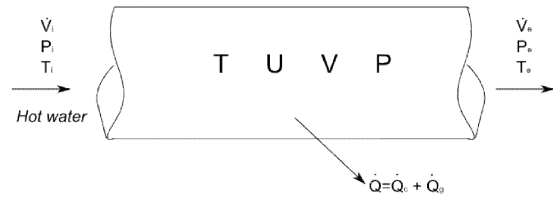


Fig. 10. Control volume

The control volume considers water transport from the inlet to the outlet of the tube and heat flow at the tube periphery. We assume homogeneous pressure, temperature and density within the control volume.

The thermal model consists of a single C-element representing the thermal capacitance of the water connected to 2-ports R-elements representing the ports at both end and a single R-element representing the dissipation of thermal energy by the conduction of heat from the tube to the concrete screed through the tube periphery.

From the PBG model of Figure 11, we deduct the equations (16), (17) from the hydraulic model (solid link) and equation (18) from the thermal model (dotted link). The hydraulic model is steady-state with the inlet volume flow rate \dot{V}_i and inlet pressure P_i set by the pump:

$$P_i = P_e \quad (16)$$

The continuity of the volume flow rate gives:

$$\dot{V}_i = \dot{V}_e \quad (17)$$

The state equation, from the dynamic thermal model can be written as follows:

$$\frac{dU}{dt} + \dot{H}_e = \dot{H}_i + \dot{Q} \quad \frac{dU}{dt} = \dot{H}_i - \dot{H}_e + \dot{Q} \quad (18)$$

where:

$$\dot{H}_i = \rho \dot{V}_i c_p T_i \quad (19)$$

$$\dot{H}_e = \rho \dot{V}_e c_p T_e \quad (20)$$

$$\dot{Q} = \dot{Q}_c + \dot{Q}_g = \frac{T - T_f}{RA} \quad (21)$$

In equation (21), R represents the internal convective thermal resistance in the tube and T_f is the temperature at the outside surface of the tube, corresponding to the half-height temperature of the floor.

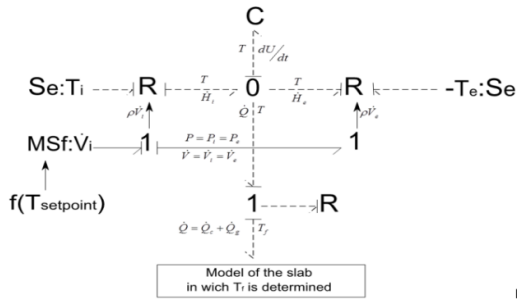


Fig. 11. Pseudo-Bond Graphs model for the hot water tube (floor heating)

Equations (17) and (18) satisfy the mass balance and the energy balance respectively. The satisfaction of the energy conservation requires one 0-junction with three links relating the two 2-ports *R* elements corresponding to the tube's inlet and outlet [26,27,28]. The other links for the two *R*-elements are connected directly at the effort (temperature) sources *Se* at inlet and outlet. The coupling between the hydraulic and thermal models is done through a signal sending value of the volumetric flow rate allowing the calculation of the thermal flow rate in the 2-ports *R* element.

There is no exchange of mechanical work with the environment since $dV = 0$. We deduce:

$$dU = \rho V c_V dT \tag{22}$$

Equation (18), based on the entries of the system and fluid properties, can be driven as follows:

$$\frac{dU}{dT} = \rho \dot{V}_i c_p T_i - \rho \dot{V}_e c_p T_e + \left(\frac{T - T_f}{RA} \right)$$

$$\frac{dU}{dT} = \rho \dot{V}_i c_p T_i - \rho \dot{V}_e c_p T_e - \left(\frac{T_f}{RA} \right) + U \left[\frac{1}{RA \rho V c_V} \right] \tag{23}$$

Equation (23) is a first order differential equation which is easily solved for *U* and the water temperature is then determined by equation (24):

$$T = \frac{U}{\rho V c_V} \tag{24}$$

This PBG model includes all three state variables, *T*, *P* and *V*, whose values are derived, for the temperature, after integration of the internal energy *U*, and for the pressure and volume, from their initial states (assumption of incompressible fluid). The dynamic model of the hydraulic system is coupled with the building envelope model, the radiation model and the inside air model.

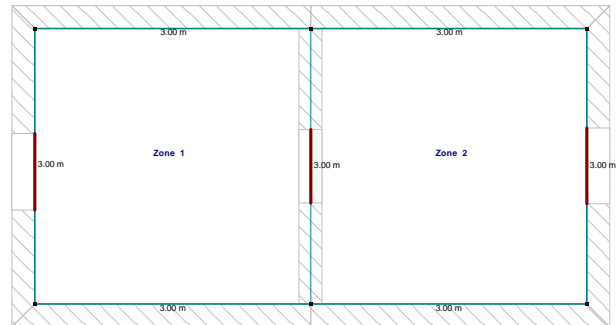
3.2 Test case

In order to validate the global Bond Graphs model, the structure we used for the comparison of our simulation is a building within the platform ENERBAT (energy efficiency of buildings) at the Faculty of Sciences and Technologies of University of Lorraine (France). This test building was set up to fit the requirements of a low energy consumption home design.

The building occupies a floor area of approximately 18 m² and has a height of 2.3 m. The structure is divided into two zones of equal size (9 m²) separated by a mobile partition. Zone 1 is equipped with a heated floor and a chilled ceiling. This RHC system can meet the need for heating (in winter) and cooling (in summer). Table 1 shows the thermo-physical properties of materials making up the envelope and the characteristics of the RHC system. We have to create adequate conditions of temperature thermal comfort.



(a)



(b)

Fig. 12. The test building (platform ENERBAT)

Table 1. Thermo-physical properties of materials

Elements	Designation	Thermal conductivity λ (W.m ⁻¹ .K ⁻¹)	Specific heat c_p (J.kg ⁻¹ .K ⁻¹)	Density ρ (kg.m ⁻³)
Walls (e = 8.4 cm)	Wood*	0.13	1600	490
	Wood* (e=6.2 cm)	0.13	1600	490
Roof (e = 20 cm)	Steel modules (e=2 cm)	61	460	7860
	Air space (e = 11.8 cm)	24.3	1004	1.29
	Concrete screed (e = 6 cm)	1.4	880	2300
Floor (e = 11.5 cm)	Polyurethane Layer (e = 5.5 cm) Only in zone1	0.03	837	35
	Hydraulic system	Tube diameter (cm)	Tube length (cm)	
RHC heating-cooling System (only in zone 1)	Floor heating	D _{ext} = 1.7 D _{int} = 1.5	6290	
	Chilled ceiling	D _{ext} = 1.2 D _{int} = 1.0	4280	

* With the moisture content of 10 % ± 3 %.

The global surface inside and outside resistances R_i and R_e , used in the simulations are exposed in table 2, taking into account the global coefficients of heat exchange. Through experimental tests, Bairo [28] developed correlations to evaluate the transient convective exchange taking place in a building wall made up of air filled cells. His study contains the data required for an extensive analysis of the thermal and dynamical behavior of building walls which may take into account joint convection-conduction modes and capacitive effects.

Table 2. Surface inside and outside resistances [28, 29]

Designation	R_i ($m^2.K.W^{-1}$)	R_e ($m^2.K.W^{-1}$)
Walls	0.13	0.04
Roof	0.10	0.04
Floor	0.17	-

The operating settings of the RHC system are shown in table 3. The PID regulation provides, according to the set temperature, the change of operation scenarios. Zone 2 is not controlled (no HVAC system in this zone).

Table 3. Operating settings of the RHC system

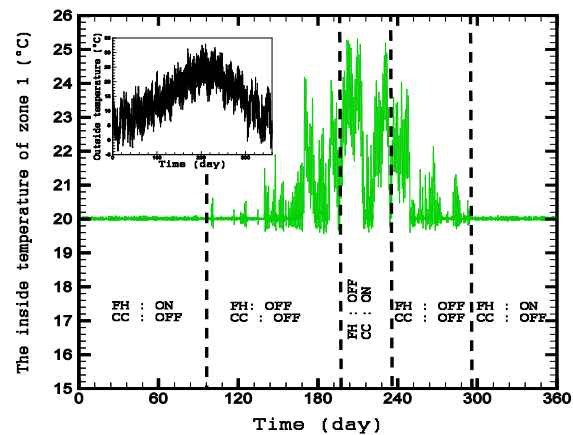
Temperature ($^{\circ}C$)	Floor heating	Chilled ceiling
$T < 20$	ON	OFF
$T > 25$	OFF	ON
$20 < T < 25$	OFF	OFF
Inlet temperature of hot water ($^{\circ}C$)	40	
Inlet temperature of cold water ($^{\circ}C$)	7	

3.3 Simulation results

The simulation results of the global model are compared with those generated by the software TRNSYS. Comparing the predictions of different approaches is quite difficult due to manner in which this simulation (modeling) tools generate mathematical models. The methodologies of the two approaches differ in terms of modeling procedure, physical expression and simulation tool. TRNSYS (TRAnnsient SYstem Simulation tool) is an extremely flexible graphically based software environment used to simulate the behavior of transient system. The indoor and surface temperatures for the two zones are calculated in order to examine the reliability of the RHC system used to supply the living space with desired conditions. In the absence of ventilation, thermal comfort should satisfy: (i) the indoor air temperature between $20^{\circ}C$ (in winter) and $26^{\circ}C$ (in summer); (ii) a radiant temperature between $19^{\circ}C$ and $27^{\circ}C$; and (iii) a relative humidity between 40 % and 70 % [30-32]. The risk of condensation is then considered. In the following, we analyze the simulation results based on the above criteria in order to assess the performance of the RHC floor heating-chilled ceiling system.

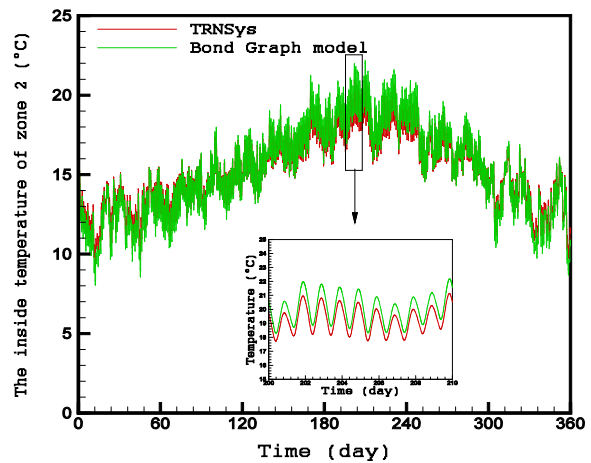
In Figure 13 indoor temperatures in the two zones, determined by our PBG model, are reported for the entire year. The weather data is provided by the local weather station. Dashed lines (Fig.10a) delimit the operating modes. The indoor temperature of zone 2 (Fig.10b) determined by our Bond Graphs model and TRNSYS has been a main part of validation for the Bond Graphs model. Those graphs are very close, with a maximum deviation of about $1^{\circ}C$ over the entire simulation period. Indoor temperature decreases significantly in winter (between $8^{\circ}C$ and $15^{\circ}C$) due to the absence of any heating system in this room, leading to thermal discomfort in this period.

The estimation of the surface temperatures for the RHC system is essential for two reasons: (i) minimizing the risk of mold deposit by controlling the surface temperature of cooling system (here the chilled ceiling) and (ii) ensuring the thermal comfort by maintaining the surface temperature of the floor at acceptable level. The thermal behavior of the RHC system need to be investigated in order to respect the above recommendations by acting on the inlet hot and cold water temperatures. Therefore, the surface temperatures have been generated by Bond Graphs model and TRNSYS for the heating floor and the chilled ceiling, respectively (Fig.14). We see that the Bond Graphs model shows the same expected thermal behavior as given by TRNSYS. The surface temperature of the heating floor does not exceed $29^{\circ}C$ in cold days (Fig.14a). For the cooling system (Fig.14b), the surface temperature is always greater than the dew point temperature, hence avoiding the risk of condensation and, in same time, insuring a good thermal comfort level. In addition, we realize that the selected cooling technique is rather more useful for cold and dry climate.



FH : Floor Heating
CC : Chilled Ceiling

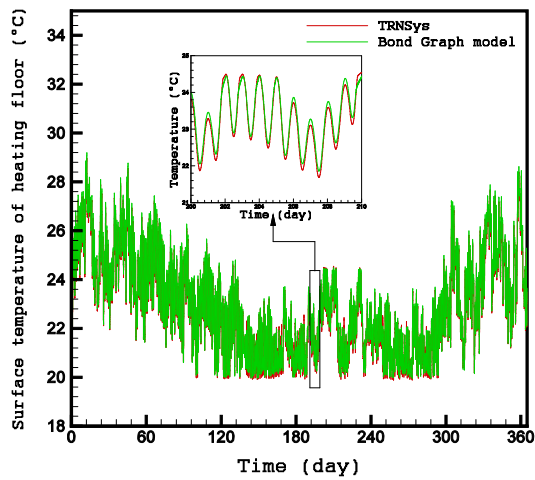
(a)



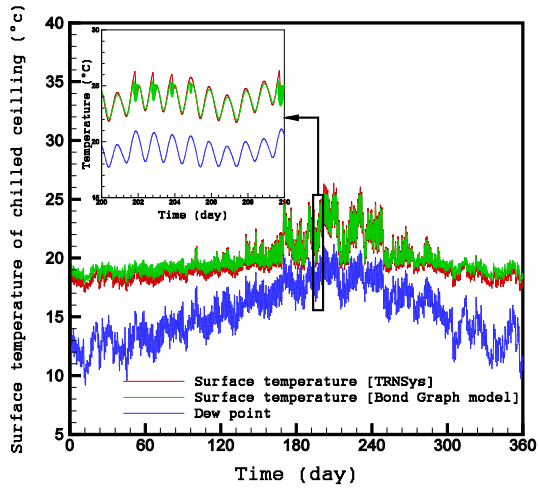
(b)

Fig. 13. Indoor air temperatures. (a) zone 1 and (b) zone 2

The heating loads calculated with the two simulation programs are presented in Figure 15. The climate in this study requires a permanent heating all year round. Primary energy consumption for the whole year is estimated at $313 kWh/m^2/year$.



(a)



(b)

Fig. 14. Surface temperatures (only zone 1). (a) Floor heating; (b) Chilled ceiling

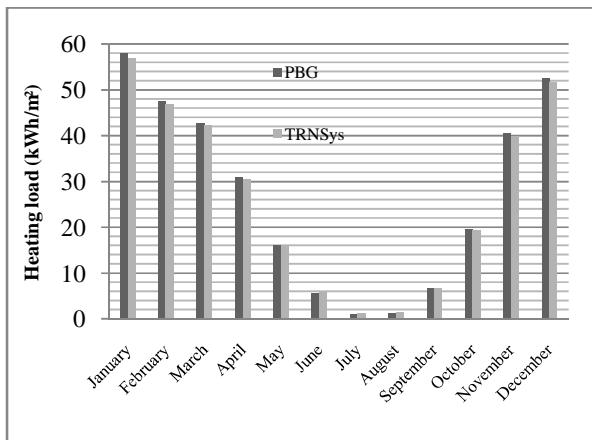


Figure 15: Heating loads for the test building

Conclusion

A building with an RHC system is investigated using the BG methodology to show the reliability of such a procedure and analyze the building thermal behavior.

The developed PBG sub-models are assembled in a building model in order to simulate and analyze the performance of the RHC system. By comparison with TRNSYS, the simulation results enhance the pertinence of the dynamic model developed in terms of the accuracy and the modeling facilities offered by the BG approach. It provides real potential for dealing with energy building system.

Using a PID regulation for controlling the indoor temperature, it appeared that zone 1 meets the criteria of thermal comfort: radiant temperature is between 19°C and 27°C and no risk for condensation. Being without HVAC system, the indoor temperature of zone 2 is low in winter.

The advantage of the RHC system, compared to conventional heating and cooling, is that it is characterized by the fact that heat and cold are distributed evenly throughout the room providing the best thermal comfort level. Another feature is that comfort is enhanced by the absence of air flow and congestion of energy devices.

References

- [1] International Energy Agency, Key World Energy Statistics, Report No 29, Paris, France, 2009
- [2] F. Chlela, Développement d'une méthodologie de conception de bâtiments à basse consommation d'énergie, Ph.D. thesis, La Rochelle University, La Rochelle, France, 2008
- [3] D.B. Crawley, J.W. Hand, M. Kummert, B.T. Griffith, Contrasting the capabilities of building energy performance simulation programs, *Proceedings*, 9th Building Simulation Conference (IBPSA'05), Montreal, Canada, 2005, Vol. 1, pp. 231–238
- [4] D.B. Crawley, Energy Plus: energy simulation program. *ASHRAE Journal*, 42(2000), 4, pp. 49–56
- [5] Lawrence Berkeley Laboratory. DOE-2 engineering manual version 2.1C. Berkeley, CA, USA, 1982.
- [6] M. Gough, Component based building energy system simulation, *International Journal of Ambient Energy*, (1986), 7, pp. 137–43. <http://dx.doi.org/10.1080/01430750.1986.9675492>
- [7] S.A. Klein, TRNSYS: A transient system simulation program, Report No. 38, Solar Energy Laboratory, University of Wisconsin-Madison, USA, 2000
- [8] K. Minoru, D. Charles, M. John, Hourly thermal load prediction for the next 24 h by ARIMA, EWMA, LR and an artificial neural network, *ASHRAE Transaction*, 101(1995), 1, pp. 186–200
- [9] F. Deque, F. Olivier, A. Poblador, Grey boxes used to represent buildings with a minimum number of geometric and thermal parameters, *Energy and Buildings*, 31 (2000), 1, pp. 29–35

- [10] B. Sohlberg, Grey box modelling for model predictive control of heating process, *Journal of Process Control*,13 (2003), 3, pp. 225–38
- [11] J.W. Brewer, P.P. Craig, P. Hubbard, K.E.F. Watt, The bond Graph method for technological forecasting and resource policy analysis,*Energy*,7 (1982), 6, pp. 505 – 537
- [12] S.H. Cho, M. Zaheer-uddin, An experimental study of multiple parameter switching control for radiant floor heating systems, *Energy*, 24(1999), 5, pp. 433 – 444
- [13] J.J.H Tsai, J.S. Gero, A qualitative energy-based unified representation for buildings, *Automation in construction*, 19 (2010), 1, pp. 20-42
- [14] N. Paynter, Analysis and design of engineering systems, MIT Press, MA, USA, 1961
- [15] B. Olesen, Radiant floor cooling systems, *ASHRAE Journal*, 50 (2008), 9, pp. 16-22
- [16] M. Amir, M. Lacroix, N. Galanis, Thermal analysis of electric heating floor panels with daily heat storage, *International journal of thermal sciences*,38 (1999), 2, pp. 121 – 131
- [17] S. Larsen, C. Filippin, G. Lesino, Transient simulation of a storage floor with a heating/cooling parallel pipe system. *Building and Simulation : An International Journal*,3 (2010), 2, pp. 105 – 115
- [18] A. Mokhtari, H. Kazeoui, Y. Boukezzi, G. Achar, Utilisation d'un circuit hydraulique dans un plancher pour le chauffage et le rafraîchissement des locaux, *Revue des Energies renouvelables*, 1 (1998), pp. 17 – 27
- [19] N. F. Diaz, Modeling of a hydronic ceiling system and its environment as energetic auditing tool, *Journal of Applied Energy*, 88 (2011), 3, pp. 636-649
- [20] A. Kebabci, N. Ghaddar, K. Ghali, Model-based optimal supervisory control of chilled ceiling displacement ventilation system, *Energy and Buildings*, 43 (2011), 43, 6, pp. 1359 - 1370
- [21] X. Hao, G. Zhang, Y. Chen, S. Zou, D. J. Moschandreas, A combined system of chilled ceiling, displacement ventilation and desiccant dehumidification, *Building and Environment*, 42 (2007),9, pp. 3298 – 3308
- [22] F.E. Cellier, A. Nebot, Bond Graphs modelling of heat and humidity budgets of Biosphere 2. *Environmental modeling and software*, 21 (2006), 11, pp. 1598-1606
- [23] W. Borutzky, Bond Graph methodology: Development and Analysis of Multidisciplinary Dynamic System Models, Springer-Verlag, London, UK, 2010
- [24] A. Merabtine, S. Mokraoui, R. Benelmir, D. Descieux, A Comparative Modeling of an Experimental Single-Zone Building with Bond Graphs and TRNSYS, *International Journal of Energy, Environment, and Economics*, 20 (2012), 1, pp. 53-73
- [25] S. Mokraoui, A. Merabtine, R. Benelmir, N. Laraqi, Bond Graph Approach for Modeling and Analysis of Transient Heat Conduction in the Prospect of Energy Building Application, *International Journal of Energy, Environment, and Economics*, 20 (2012), 1, pp. 39-52
- [26] D.C. Karnopp, R.L. Margolis, R.C. Rosenberg, System dynamics: Modeling and Simulation of Mechatronic Systems, Wiley, New York, USA, 2005
- [27] D. Karnopp, S. Azarbaijani, Pseudo Bond Graph For generalized Compartmental Models in engineering and physiology, *Journal of Franklin Institute*, 312 (1981), 2, pp. 95 – 108
- [28] D. Karnopp, State variables and Pseudo Bond Graphs for compressible thermofluid systems, *Journal of dynamic systems, measurement, and control*, 101 (1979), 3, pp. 201 – 204
- [29] D. Karnopp, Pseudo Bond Graphs for thermal energy transport, *Journal of dynamic systems, measurement, and control*, 100 (1978), 3, pp. 165 – 169
- [30] F. Doumenc, Élément de thermodynamique et thermique, http://www.fast.usud.fr/~doumenc/la200/CoursThermodynamique_L2.pdf
- [31] A. Baïri, Transient free convection in passive buildings using 2D air-filled parallelogram-shaped enclosures with discrete isothermal heat sources, *Energy and Buildings*,43 (2011), 2-3,pp. 366-373
- [32] Réglementation Thermique 2005. Guide réglementaire 2005. CSTB.
- [33] M. Weiner, Modeling and simulation of a solar energy system. A research report, Department of Electrical and computer Engineering, University of Arizona, 1992
- [34] A. Baïri, N. Laraqi, J.M. García de María, Numerical and experimental study of natural convection in tilted parallelepipedic cavities for large Rayleigh numbers, *Experimental Thermal and Fluid Science*, 31(2007), 4, pp. 309-324
- [35] M. Santamouris, C. Pavlou, P. Doukas, G. Mihalakakou, A. Synnefa, A. Hatzibiros, P. Patargias, Investigating and analysing the energy and environmental performance of an experimental green roof system installed in a nursery school building in Athens, Greece, *Energy*, 32 (2007), 9, pp. 1781 – 1788
- [36] A. Baïri, N. Laraqi, J.M. García de María, Importance of radiative heat exchange in 2D closed diode cavities applied to solar collectors and building, *International Journal of Sustainable Energy*, 24 (2005), 1, pp. 33-44
- [37] D. Medjelekh, S. Abdou, M. El Ganaoui, Impact of the Thermal Inertia of Material on the Hygrothermal Comfort of Building, *International Review of Chemical Engineering*, 2 (2010), 3, pp. 391-397